Herpesvirus chemokine binding protein gG efficiently inhibits neutrophil chemotaxis *in vitro* and *in vivo*

Gerlinde R. Van de Walle, Maeva L. May, Woraporn Sukhumavasi, Jens von Einem & Nikolaus Osterrieder

Department of Microbiology and Immunology, College of Veterinary Medicine, Cornell University, Ithaca, NY 14853

Running title: Herpesvirus glycoprotein G inhibits neutrophil chemotaxis

Keywords: viral infections, chemokines, chemotaxis, neutrophils

Abstract

Glycoprotein G (gG) of alphaherpesviruses has been described to function as a viral chemokine binding protein (vCKBP). More recently, mutant viruses devoid of gG have been shown to result in increased virulence, but it remained unclear if gG's potential to serve as a vCKBP is responsible for this observation. We here used equine herpesvirus type 1 (EHV-1) as a model to study the pathophysiological importance of vCKBP activity. First, *in vitro* chemotaxis assays studying migration of immune cells, an important function of chemokines, were established. In such assays, supernatants of EHV-1-infected cells could significantly inhibit IL-8-induced chemotaxis of equine neutrophils. Identifying gG as the responsible vCKBP was achieved by repeating similar experiments with supernatants from cells infected with a gG-negative mutant. These supernatants were unable to alter IL-8-induced equine neutrophil migration. Furthermore, recombinant EHV-1 gG was able to significantly reduce neutrophil migration, establishing gG as a bona fide vCKBP. Secondly, and importantly, *in vivo* analyses in a murine EHV-1 infection model showed that neutrophil migration in the target organ lung was significantly reduced in the presence of gG. In summary, we demonstrate for the first time that EHV-1 gG not only binds to chemokines but is also capable of inhibiting their chemotactic function both *in vitro* and *in vivo*, thereby contributing to viral pathogenesis and virulence.

Introduction

Recently, gG of several alphaherpesviruses has been described to function as a broad-spectrum chemokine binding protein [1,2]. As chemokines play central roles in mediating inflammatory responses during viral infection, it is not surprising that viruses have adopted strategies to evade or modulate chemokine activity. Currently, three viral strategies of chemokine modulation are described, all of which are well studied in both herpes- and poxviruses [3-5]. First, viruses can encode open reading frames with striking homology to genes that encode chemokines. These so-called virus-encoded chemokine homologues or virokines can act either as agonists or antagonists of host molecules. For example, the alphaherpesvirus Marek's disease virus (MDV) has been shown to encode a biologically active IL-8 homologue [6]. MDV vIL-8 showed significant similarities with mammalian and chicken IL-8 homologues, with the exception of a highly conserved ELR motif which is absent from the molecule. *In vitro* chemotaxis studies demonstrated that vIL-8 attracts chicken mononuclear cells, and *in vivo* studies with vIL-8 deletion mutants showed a significantly decreased level of lytic infection and virulence [6]. Second, a remarkable number of viral genes have been identified to resemble cellular genes encoding chemokine receptors and have been shown to engage chemokines and induce intracellular signals. Third, several poxviruses, and, more recently, alphaherpesviruses have been shown to express soluble vCKBP that do not share sequence similarity with known chemokines or chemokine receptors.

EHV-1, a member of the *Alphaherpesvirinae* and a close relative to the causative agents of cold sores and genital herpes in humans, HSV-1 and HSV-2 respectively, is a major pathogen of horses worldwide. EHV-1 is spread via nasal secretions and replicates in the respiratory tract. Initial replication in airway epithelia is followed by a leukocyte-associated viremia, which

enables EHV-1 to reach end-vessel endothelia in the uterus and central nervous system. In these organ systems, viral replication can result in vasculitis and perivasculitis ultimately resulting in abortion and reactive myeloencephalophathy, a highly lethal condition of enormous economic and public health importance [7]. A related alphaherpesvirus in horses, EHV-4, is predominantly associated with respiratory disease [8,9]. Both viruses encode glycoprotein G, a type I integral membrane protein. The N-termini of EHV-1 and EHV-4 gG exhibit high sequence similarity, whereas the extracellular C-terminal domains are highly divergent [10]. Glycoprotein G is expressed early in the infectious cycle and was shown to be nonessential for virus growth *in vitro* [11-13]. Moreover, gG is unusual in that it can exist in three isoforms: a 68-kDa full-length membrane-bound form, a 12-kDa membrane-bound form, and a 60-kDa form, which is secreted from infected cells [14]. The latter two isoforms appear to be the result of a proteolytic event from the 68-kDa full-length form resulting in the 12-kDa C- and the 60-kDa N-terminal moiety, respectively.

Since EHV-1 gG has been shown to bind a broad range of chemokines of human and murine origin, this glycoprotein has also been implied to function as a vCKBP [1]. More recently, our group constructed a mutant virus devoid of gG, which was tested in a murine EHV-1 infection model. It was observed that infection with such gG-negative virus resulted in increased pathogenicity in mice [13]. It remained unclear, however, whether the virulence mechanism of this EHV-1 mutant virus was caused by the absence of vCKBP activity. In the present study, we used EHV-1 as a model to investigate in more detail the pathophysiological importance of gG binding to chemokines. Chemotaxis assays with equine leukocytes and equine chemokines were performed *in vitro*, and EHV-1 gG was compared to the action of its counterpart in EHV-4, a close relative of EHV-1. Moreover, the *in vivo* relevance of chemokine binding by gG was

tested in a murine infection model. The salient findings of our study are that gG of EHV-1 is not only capable of inhibiting the function of chemokines, such as IL-8, in neutrophil migration *in vitro*, but also has a significant effect on migration of immune cells in the target organ *in vivo*. This report, therefore, is the first to link gG binding to chemokines with a virulence phenotype *in vivo* and this may indicate an important role of gG in viral immune evasion in alphaherpesvirus infection.

Materials & Methods

Cells. Rabbit kidney cells (RK13) or equine fibroblasts (NBL6) were grown and maintained in growth medium (MEM supplemented with 10% FBS, 100 U/ml penicillin and 0.1mg/ml streptomycin) at 37°C under a 5% CO_2 atmosphere.

Equine neutrophils were isolated by density centrifugation of heparinized blood from healthy horses on a discontinuous Percoll gradient as described previously [15]. After washing, cells were resuspended in MEM at $1X10^5$ cells/ml and used immediately for further experimentation. Equine PBMC were isolated using Histopaque 1077 (Sigma) following the manufacturer's instructions. After two washing steps, cells were resuspended in MEM at $1x10^5$cells/ml and used immediately for further experimentation. To obtain a pure equine monocyte population, PBMC were resuspended in leukocyte medium [RPMI1640 (Invitrogen) supplemented with 10% FBS, 0.3mg/ml glutamine, 100U/ml penicillin, 0.1mg/ml streptomycin, 1mM sodium pyruvate and 1% non-essential amino acids (Invitrogen)], at $2x10^6$ cells/ml. Cells were seeded in polystyrene tissue culture dishes and cultivated at 37°C under a 5% CO_2 atmosphere. After 24h of incubation, non-adherent cells mainly representing lymphocytes were removed by washing the culture dishes with RPMI 1640, and adherent monocytes were centrifuged, washed and resuspended in MEM at a density of $1X10^5$cells/ml. Murine neutrophils were isolated from Balb/c mice by peritoneal lavage as described before [16]. The purity of each cell population was confirmed on cytospins with modified Wright stain (Sigma).

Viruses. EHV-1 wild-type strain RacL11, the gG deletion mutant (vL11ΔgG) and the gG rescuant virus (vL11ΔgGR) were described previously [13,17]. An EHV-4 isolate (VLS#829) was kindly provided by the OIE reference laboratory at the University of Kentucky and was identified as EHV-4 by RFLP of its virus DNA (data not shown). Stocks of EHV-1 and EHV-4

were produced in RK13 or NBL6 cells. For infection experiments, cells were washed twice with MEM and inoculated for 24h with virus at a multiplicity of infection (MOI) of 1 in growth medium. At 24h post infection (p.i), supernatants from infected cells were collected. Virus and cellular debris was removed from supernatants by centrifugation at 100,000xg for 1h and cleared supernatants were subsequently used in chemotaxis assays.

Western blotting. Western blot analyses were performed essentially as described [13]. To detect gG, polyclonal rabbit anti-gG antibodies (1:500) were used that recognize the variable domain of gG of EHV-1 or EHV-4 (both antisera were kindly provided by Drs. M. J. Suddert and C. Hartley) [12]. Penta-His antibodies were obtained from Qiagen (Valencia, CA) and used to detect His-tagged proteins. Anti-mouse (1:7,500) or anti-rabbit (1:5,000) immunoglobulin G (IgG) peroxidase conjugates were from Jackson Immunoresearch Laboratories.

Plasmids. The pRacL11 bacterial artificial chromosome (BAC) clone has been described previously [18]. pRacL11 DNA was isolated using the Maxi-prep kit (Qiagen) and used as a template to amplify by PCR a portion of the gG gene that would encode a truncated, secreted version of the viral protein. The SignalP prediction server (version 1.1) was used to predict signal peptide cleavage sites and membrane-spanning segments. Based on the predictions, a fragment of 1,020 bp within the gG gene encoding the extracellular portion of gG was amplified by conventional PCR introducing *Cpo*I sites at either end using gGFCpoI and gGRCpoI primers (Table I), and then inserted into pBac11 (Novagen, Madison, WI) (pBac11sgG). This cloning strategy fused 1) the extracellular domain of gG in-frame with the baculovirus gp64 signal peptide present in pBac11, and 2) added a polyhistidine tag to the carboxyterminus of secreted gG (Histag) (Figure 1). The pBac11sgG clones were analyzed by DNA sequencing and subsequently electroporated into DH10Bac cells (Invitrogen) harboring the baculovirus BAC

sequence and allowing T7-mediated transposition of gG sequences into the targeted locus of baculovirus DNA. The sequence of equine CCL2 [19] was codon-optimized, synthesized, and cloned into the pLS vector (TOP Gene Technologies, Montreal, Canada). Cloning of equine CCL2 (300bp) into the pBac11 vector was performed exactly as described for gG but using primer pair CCL2FCpoI and CCL2RCpoI (Table I). Transposition after transformation of DH10Bac cells was done as described above.

Baculovirus expression and protein purification. Recombinant baculovirus bacmid DNA encoding His-tagged secreted gG (sgG-His) or equine CCL2 (eCCL2-His) were transfected into Sf9 insect cells using Celfectin (Invitrogen). Recombinant viruses were plaque purified twice and verified for expression by western blotting with antibodies against gG and/or the polyhistidine tag. For purification of sgG-His or eCCL2-His from supernatants of baculovirus-infected Sf9 insect cells (MOI of 1.0), TALON resin (Clontech, La Jolla, CA) was used, exactly as described previously [20]. Fractions containing His-tagged proteins were collected and their purity was determined by SDS-PAGE, followed by Coomassie Blue staining. Protein concentration was determined with a Bradford assay following the manufacturer's instructions (Biorad).

Chemotaxis assays. For chemotaxis assays, 12-well Costar Transwell plates were used (Corning Costar Co., Cambridge, MA). Serial dilutions of chemokines were made in MEM. Recombinant equine IL-8 and mouse KC were obtained from Serotec (Kidlington, Oxford, UK). Recombinant equine CCL-2 was produced as described above. Chemokines were pre-incubated for 30min at 37°C with serial dilutions of viral gG, either present in supernatants of infected cells or recombinantly expressed, and 600µl of each dilution was applied to the lower chambers of the wells. Wells were covered with a polycarbonate membrane with a 3µm pore size for neutrophils

and a 5μm pore for mononuclear cells. A 100μl cell suspension (containing $1x10^4$ cells) was added to the top chamber and assay plates were incubated at 37°C for 45min for neutrophils and 2h for mononuclear cells. Dilutions of chemokine and medium alone were included in each experiment to serve as positive and negative controls, respectively. After incubation, cells in the lower chamber were stained, counted under a light microscope (Zeiss Axiovert 25) and expressed as % chemotaxis based on the amount of input cells, unless indicated otherwise.

Animal experiments. These animal experiments were performed in accordance with the United States Animal Welfare Act, under the supervision of the Cornell Institutional Animal Care and Use Committee, and were conducted as described previously with some modifications [21]. Briefly, 4-week-old female BALB/c mice (16 mice per group) were infected with vL11ΔgG or vL11ΔgGR by the intranasal route at $4x10^4$ PFU/mouse. Virus was suspended in 20μl of cell growth medium. Control mice were infected with growth medium alone. Individual weights of mice were determined on the day of infection (day 1) until day 14 and percentages of body weight loss were determined. Two mice in each group were euthanized to collect the lungs. These extracted lungs were homogenized to determine virus titers by standard titration on RK13 cells. On day 1, 2, 4 and 14 p.i., 4 mice in each group were euthanized and inflammatory cells infiltrating the airways were harvested by BAL exactly as described previously [22]. BAL cells were washed twice and finally resuspended in 1ml ice-cold PBS. Total cell numbers were determined based on amount of recovered BAL fluid. To analyze the differential cell counts, both cytospins and flowcytometric analyses were performed. Cytospins were obtained by centrifuging 100μl of the cell suspension onto microscope slides at 700 rpm for 4min. Cytospins were air dried and stained with modified Wright stain (Sigma). In total, at least 300 cells per

BAL were counted by light microscopy and the different immune cells and their absolute numbers were determined.

Flow cytometric analysis. To analyze the composition of immune cells in the airways of lungs of infected animals, BAL were stained with fluorescently labeled rat-anti-mouse monoclonal antibodies against a surface marker on neutrophils (Gr-1^+-PerCP, BD Biosciences, San Diego, CA), on macrophages (F4/80-ACP, Invitrogen, Carlsbad, CA), on B lymphocytes (B220-PE, BD Biosciences) and various surface markers on T lymphocytes (CD3-ACP and CD4-FITC from eBioscience, San Diego, CA & CD8-PECy7 from BD Biosciences). All antibodies were used at a final concentration of 2μg/ml, with the exception of the Gr-1^+-PerCP which was used at 1μg/ml. Cells were incubated with ammonium chloride for 1min at RT to lyse erythrocytes (red blood cell lysis buffer Hybri-Max, Sigma) and then pre-incubated with normal mouse serum for 30min at 4°C to block Fc receptors. Subsequently, cells were stained with labeled antibodies for 15min at 4°C against cells of the innate immune system one the one hand and against cells of the adaptive immune system on the other hand. After two wash steps, flow cytometric analysis was performed and individual cell populations were identified according to the presence of specific fluorescence-labeled antibody. All analyses were performed with an acquisition of at least 10,000 events on a Becton Dickinson FACSCalibur flow cytometer (BD Biosciences), and the data were analyzed using Cell Quest software (BD Biosciences, San Jose, CA).

Results

Chemotaxis assays studying IL-8-induced migration of equine neutrophils. Recently, secretion of vCKBP's by alphaherpesviruses, including the equine alphaherpesvirus EHV-1, was described. Using radiolabeled human and murine chemokines in cross-linking assays, the formation of chemokine-vCKPB complexes with EHV-1 gG was demonstrated [1]. To investigate if gG-chemokine complex formation also is functionally important and to assess the putative mechanism of vCKBP action, chemotaxis assays were established using equine immune cells and the equine chemokine IL-8. This type of assay was selected because chemokines play a key role in the directional attraction of immune cells during infection [23]. IL-8 was chosen as the preferential chemokine as human IL-8 has been described to form a complex with EHV-1 gG [1]. As shown in Figure 2, equine neutrophils readily migrated in response to recombinant equine IL-8. Around 37% of neutrophils migrated along the cytokine gradient when 10ng/ml IL-8 were used and migration increased up to 52% in the presence of 50ng/ml of IL-8. Similar results were observed using equine basophils (data not shown). However, when using equine PBMC in the chemotaxis assay, no cell migration could be observed for all concentrations tested (Figure 2), indicating the specificity of the equine molecule for cells of the neutrophil lineage.

Supernatants of EHV-1-infected cells inhibit IL-8-induced chemotaxis of equine neutrophils. To study the possible interference of the EHV-1 vCKBP with the migration of immune cells *in vitro*, IL-8 was pre-incubated with 300µl of supernatant from EHV-1-infected cells for 30min before performing the chemotaxis assay. The supernatants had been cleared of all cell debris and virus particles by ultracentrifugation, and, therefore, only proteins secreted from the infected cells were used as a protein source in the assays. As shown in Figure 3, a significant reduction up to 50% in the migration of equine neutrophils was observed in the

presence of supernatant of EHV-1 infected cells ($p<0.05$). The supernatant by itself did not have any effect on equine neutrophil migration under unstimulated conditions (data not shown).

Viral glycoprotein G (gG) of EHV-1 is responsible for the inhibition of IL-8-induced chemotaxis. To determine if gG in the supernatants of EHV-1-infected cells was responsible for the reduction of IL-8-induced chemotaxis, the assays were repeated with supernatants of cells that had been infected with a gG deletion mutant (vL11ΔgG). As a control, supernatants of cells infected with a rescuant virus (vL11ΔgGR), in which gG expression was restored, were also included. These viruses had been intensively characterized both *in vitro* and *in vivo* in a previous study [13]. First, Western blot analysis using polyclonal antibodies directed against EHV-1 gG demonstrated indeed the presence of secreted gG as a 55-60-kDa protein in supernatants of wild type- and vL11ΔgGR-infected cells (Figure 4A). As expected, no secreted gG was present in the supernatant of mock- and vL11ΔgG-infected cells (Figure 4A). Interestingly, supernatants of vL11ΔgG-infected cells, devoid of secreted gG, did not alter the neutrophil migration in the chemotaxis assay when compared to IL-8 alone (Figure 4B). In contrast, supernatants of cells infected with wild-type or the gG rescuant virus, both of which contained secreted gG, were shown to significantly reduce neutrophil migration (Figure 4B), similar to the observation documented in Figure 3. These results were a strong indication that secreted gG functions as the vCKBP responsible for the interference with neutrophil chemotaxis. Finally, to clearly identify gG as the vCKBP and also to exclude possible interactions of other viral and/or cellular proteins secreted from cells with chemokine-mediated attraction of neutrophils, the secreted form of EHV-1 gG was expressed in insect cells using a baculovirus expression system. A 6xHis tag was introduced to facilitate purification of sgG by resin affinity chromatography. Coommasie blue staining of fractions eluted from the affinity column revealed a major protein of around 58-

kDa present in fractions 2 and 3 (Figure 5A). Western blot analyses of sgG-His using EHV-1 gG-specific polyclonal antibodies showed a major protein band of around 58-kDa and also a minor band of 130-kDa, possibly representing sgG-His dimers (Figure 5A) [24]. Western blot analysis with anti-Penta-His antibodies was also performed and gave identical results, i.e. proteins of 58- and 130-kDa in size were detected (data not shown). When performing the IL-8 chemotaxis assays using 50ng/ml IL-8 and serial dilutions of sgG-His, we observed a significant reduction in cell migration, which reached a plateau of 78±5.2% reduction, starting at 0.6μg/ml of sgG-His (Figure 5B). These data confirmed the importance of EHV-1 gG for inhibition of IL-8-induced chemotaxis and, therefore, its identity as a major, physiologically and functionally important vCKBP.

EHV-1 and EHV-4 are two closely related viruses with sequence similarities of proteins reaching 80%, and, most importantly, the gG's of both viruses share a high sequence identity of 72% [10,25]. Despite the similarities between the viral genomes, EHV-4 is unable to induce a systemic infection and remains confined to the upper respiratory tract. We tested in our chemotaxis assay whether anti-chemotactic activity was observed when supernatants of EHV-4-infected cells were used [1]. The chemotaxis assays using recombinant equine IL-8 and supernatants of EHV-4-infected cells revealed that no significant interference with neutrophil migration was observed (Figure 6A). This failure to block neutrophil migration was not caused by an absence of EHV-4 gG, as confirmed by western blot analysis using polyclonal antibodies directed against EHV-4 gG (Figure 6B). The antibody is specific for EHV-4 gG and did not recognize gG of EHV-1, consistent with results obtained in previous studies [12] (Figure 6B). These results clearly indicated that gG of EHV-4, despite high sequence and structural similarity with its EHV-1 counterpart, does not exhibit properties consistent with a vCKBP interfering with

at least IL-8-induced chemotaxis. This observation may be of great interest in the light of the different life styles of EHV-1 and EHV-4 gG and might at least in part explain the failure of the latter to result in systemic infections [9].

Glycoprotein G of EHV-1 does not inhibit CCL2-induced chemotaxis of equine monocytes *in vitro*. It was demonstrated that an excess of human CCL2 is unable to competitively inhibit binding of EHV-1 vCKBP to IL-8, implying that the vCKBP does not bind CCL2 [1]. We here examined whether EHV-1 gG could interfere with CCL2-induced chemotaxis. As equine CCL2 was not commercially available, recombinant, His-tagged equine CCL2 was expressed in insect cells using a recombinant baculovirus system. The equine CCL2 sequence introduced into the baculovirus genome was based on the published equine CCL2 sequence [19]. The presence of CCL2-His in the supernatant of insect cells infected with the CCL2-expressing baculovirus was demonstrated by western blot analysis using Penta-His antibodies (Figure 7A). Its biological activity was shown in a chemotaxis assay where CCL2 was able to attract equine monocytes in a dose-dependent fashion and dependent on the input of cells, the maximum percentage of chemotaxis of monocytes in response to equine CCL2 was around 32±5.2%, using 300µl of supernatants of Sf9 insect cells expressing equine CCL-2 (Figure 7B). The activity of equine CCL-2 decreased at higher amounts of supernatant, which is consistent with previous reports that chemokine receptors are downregulated after full saturation [26]. Pre-incubation of equine CCL2 with 0.6µg/ml sgG-His for 30min, however, did not alter CCL-2-induced migration of monocytes, indicating that the vCKBP of EHV-1 indeed does not interfere with the biological function of CCL2 in monocyte recruitment (Figure 7C).

Viral glycoprotein G (gG) of EHV-1 interferes with neutrophil migration *in vivo*. In the final set of experiments, we tested the relevance of expression of EHV-1 gG, with emphasis on

neutrophil migration, in a murine model of EHV-1 infection. First, *in vitro* chemotaxis assays were performed to determine if gG is able to interfere with murine neutrophil migration. As no mouse homologue of IL-8 has been described, we used murine KC, a potent murine neutrophil attractant, in our chemotaxis assay [27,28]. Murine neutrophils migrated in response to KC (0.1µg/ml) and migration was significantly reduced in the presence of EHV-1 gG (Figure 8A, $p<0.05$), indicating that gG can intefere with KC-induced murine neutrophil migration *in vitro*. After confirming EHV-1 vCKBP activity on murine neutrophils *in vitro*, BALB/c mice were infected intranasally with $4x10^4$ PFU of vL11ΔgG or the revertant virus vL11ΔgGR, in which expression of gG had been restored. After infection, mice were monitored daily for clinical signs of infection and body weight loss. Infected mice in both groups started to lose weight as early as day 1 post infection, which continued to day 4 p.i, and reached pre-infection weights by day 10. However, throughout the whole observation period, mice infected with the gG deletion mutant vL11ΔgG lost more weight (statistically significant on day 3 and 4 p.i) and recovered less rapidly compared to the group infected with the rescuant virus vL11ΔgGR (Figure 7A). Also, virus titers were determined in lungs of infected mice on day 1, 2 and 4 p.i. At day 1 and 2 p.i., viral lung titers in mice infected with the vL11ΔgG were indistinguishable from titers of vL11ΔgGR-infected mice ($p>0.05$), indicating that during the first 2 days of infection, gG is completely dispenable for EHV-1 replication in the lungs (Figure 7B). At day 4 p.i., when declining viral titers indicated a clearance of the virus, the gG deletion mutant replicated at higher titers than the wild type ($p<0.05$), most likely indicating a delay in viral clearance in the absence of gG (Figure 7B). These findings were consistent with our previous data in which mice infected with the gG deletion mutant, especially at lower ($<10^5$) doses of infection, (i) displayed a more pronounced weight loss and (ii) showed identical viral lungs titers during the early phase of infection [13]. At

days 1, 2, 4 and 14 p.i., mice from each group were sacrificed to collect the inflammatory cells infiltrating the airways by BAL. As shown in Figure 8B, the total amount of BAL cells differed significantly between groups. Compared to the control group, significantly more immune cells could be recovered from lungs from infected mice at day 1, 2 and 4 p.i. At day 14 p.i. the amount of BAL cells from infected mice had dropped drastically and was indistinguishable from levels of mock-infected mice. Total numbers of BAL cells were increased to approximately 200% in lungs harvested from mice infected with the gG deletion mutant vL11ΔgG when compared to vL11ΔgGR-infected mice at the early times p.i. (Figure 8B, $p<0.05$). Cytospins were prepared, which showed that macrophages and mainly lymphocytes were the predominating cell types in the lung airways of mock-infected control mice whereas neutrophils covered less than 5% of total cells (data not shown). Within 1 day of EHV-1 infection, neutrophil counts rose sharply, and, thereafter, returned rapidly to pre-infection levels starting at day 4 p.i. At days 1 and 2 p.i., neutrophil counts in mice infected with the gG deletion mutant were between 3- and 4-fold higher compared to vL11ΔgGR-infected mice (Figure 9A). The statistically significant difference ($p<0.01$) between these two groups demonstrated that viral gG interfered with neutrophil influx in the target organ, the lung, during EHV-1 infection. To examine more closely and to quantify the phenotypes present in the airways of infected lungs, BAL cells were also analysed by flowcytometry. At day 2 p.i., the percentage of neutrophils was increased upon infection compared to mock-infected mice and the percentage of neutrophils of mice infected with the gG deletion mutant reached up to 24.4%, whereas in vL11ΔgGR-infected mice neutrophil percentages remained lower and did not exceed 11.6% (Figure 9B). Also the percentage of macrophages was clearly increased compared to mock-infect animals, but for this cell type no difference was observed in BAL cells of animals infected with the gG deletion

mutant when compared to those infected with gG expressing virus vL11ΔgGR at that particular time point p.i. (Figure 9B). At day 4 p.i., however, the percentage of macrophages was significantly higher in vL11ΔgG- infected mice compared to mice infected with vL11ΔgGR, indicating that viral gG can also modulate migration of macrophages in lungs of infected mice (data not shown). All these results confirm those obtained after the microscopic inspection of the BAL cells. For B cells and T cells, no difference could be observed between BAL of vL11ΔgG- and vL11ΔgGR-infected mice at 2 days p.i. (Figure 9B). In addition, no difference could be observed in the CD4+/CD8+ T cell subpopulations both within the T cell population as between the different groups of mice: 50% $CD4^+$ versus 50% $CD8^+$, 46.6% $CD4^+$ versus 53.4% $CD8^+$ and 48.1% $CD4^+$ versus 51.9% $CD8^+$ for mock-infected, vL11ΔgGR- and vL11ΔgG-infected mice respectively.

Discussion

In several members of the large family of herpesviruses, open reading frames were identified, which encode vCKBP, capable of binding to chemokines with high affinity. Viral gG was identified as the vCKBP produced by some of the alphaherpesviruses, including EHV-1, and it had been proposed as both a chemokine modulator and possibly an entry receptor into immune cells in its membrane-bound form [1]. Moreover, recent studies using a mutant virus devoid of gG, identified viral gG as a virulence factor *in vivo* [13,29]. Since (i) binding of vCKBP's to target molecules does not necessarily imply functional activity, and (ii) it had never been investigated thus far if the viral function of gG as a vCKPB was responsible for the different phenotypes observed *in vivo*, we aimed at investigating the pathophysiological importance of gG binding to chemokines both *in vitro* and *in vivo*. Here, we could demonstrate for the first time that gG of an alphaherpesvirus not only functions as a vCKBP *in vitro*, but also has a significant effect *in vivo* as demonstrated by the reduction of the recruitment of immune cells to sites of infection, thereby significantly altering the inflammatory response of the host.

The equine alphaherpesviruses EHV-1 and EHV-4 were used as model organisms, and *in vitro* chemotaxis assays with equine leukocytes and equine chemokines were first established. Chemotaxis assays were carried out to study the functional role of vCKBP, as the attraction of immune cells is a significant property of chemokines determining the outcome of viral infections[4]. We mainly focused on IL-8-induced chemotaxis of equine neutrophils because (i) human IL-8 has been described to bind to gG of EHV-1 [1] and (ii) viral infections, including those by EHV-1, have been shown to be regularly accompanied by an upregulation of cellular IL-8 production [30-32]. We were able to demonstrate that equine neutrophils, but not equine PBMC, readily migrated in response to recombinant equine IL-8. This cell type-specific attraction is due

to the tri-amino acid motif ELR present in equine IL-8, which is essential for the specific recruitment of neutrophils and is found in most IL-8-like molecules, with some notable exceptions such as the potent B-cell chemoattractant, viral vIL-8, encoded by Marek's disease virus [6,23,33]. When chemotaxis assays were performed in the presence of supernatants of EHV-1-infected cells, a significant inhibition of neutrophil migration was observed and additional experiments unequivocally identified secreted EHV-1 gG as the factor responsible for inhibition of neutrophil chemotaxis. Interestingly, when using supernatants of cells infected EHV-4, a close relative of EHV-1, no inhibition of neutrophil chemotaxis was observed despite the presence of secreted gG. Future experiments are needed to determine the reason for this discrepancy in biological function. We currently hypothesize that the extracellular part of EHV-1 gG in close proximity to the membrane anchoring region is important for binding to chemokines and hence, inhibition of chemotaxis. Our hypothesis is based on the observation that approximately 100 aa of the extracellular part of EHV-4 and EHV-1 gG, adjacent to the transmembrane domain, are highly divergent and possess strong type-specific epitopes [10]. Regardless, linking the observations that (i) EHV-1 gG shows vCKBP properties whereas gG of EHV-4 does not, with (ii) EHV-1 can lead to multi-organ clinical signs whereas EHV-4 is predominately associated with mild upper respiratory disease in the natural host [8,9], makes it feasible to consider that the ability of alphaherpesvirus's gG to interfere with chemokine action might contribute to virulence and wide organ dissemination. One may speculate that the inability of gG to stop the first line of the host's defense, likely in concert with a less productive replication in the airways when compared to EHV-1 [9], may help confine the virus to upper airways.

Another important feature of gG of alphaherpesviruses is the induction of a strong antibody response upon infection (Crabb and studdert, 93; crabb et al, 95), so one might consider the effect of antibodies against gG for its proper vCKBP. Preliminary *in vitro* data seem to indicate that the inhibitory effect of gG on neutrophil migration declines in the presence of EHV-1 hyperimmune serum (personal communication, Van de Walle GR) and future experiments are necessary to study in more detail the effect of anti-gG antibodies on the vCKBP. Regardless, the interference of antibodies with a proper vCKBP function of gG might have its repercussion on the rational design of efficacious and safe vaccines. Recently, an EHV-1 mutant in which gG is deleted has been proposed as a useful marker vaccine to make a distinction between vaccinated and infected horses (Huang, 2005). This approach could raise some concerns if antibodies against gG indeed dempen the vCKBP function of gG and hence, might prevent the virus from evading the immune system.

Besides studying IL-8-induced chemotaxis of equine neutrophils and the implication on this process by the vCKBP gG of EHV-1, we also evaluated the effect of EHV-1 gG on the functionality of a chemokine that was shown not to be bound by gG **(Bryant et al.)**. CCL-2 was chosen as this is the only chemokine amongst the non-binding chemokines described by Bryant et al. that has been identified in the horse to date. After expressing CCL-2 with the baculovirus system, based on the published sequence of equine CCL-2 **(ref 19!)**, its functionality in a chemotaxis assay was demonstrated as CCL-2 was able to attract equine monocytes in a dose dependent manner. However, EHV-1 gG was not able to interfere with this CCL-2-induced chemotaxis. These data therefore indicate that an observed binding or non-binding of viral gG to chemokines can be translated into a functional interference of viral gG with chemokine-induced chemotaxis.

To address the biological importance of interference of EHV-1 gG with chemokine signaling, we used a murine model of EHV-1 respiratory disease to analyze the influx of inflammatory cells infiltrating the main target organ, the lung. First, functional interference of viral gG with murine chemokines was demonstrated in our *in vitro* chemotaxis assay using murine KC. Next, at several time points during the acute phase of EHV-1 infection, BALs were performed on mice, which had been infected with either a gG-negative deletion mutant or the gG expressing revertant virus. The rationale for performing BALs was to facilitate examination of the different types of immune cells migrating into the airways and to correlate cellular influx with severity in disease development: in diffuse lung disease caused by virus infection and other noxae, cytology of BAL correlates well with lung immunocytology [34]. The *in vivo* experiments showed that, following EHV-1 infection, a significant increase in total cell numbers in BALs was observed when compared to control mice. The majority of infiltrating cells were macrophages and lymphocytes, but at day 1 post infection, a sharp and transient increase in neutrophil counts was evident. These data are in line with immunohistological studies of EHV-1-infected murine lung tissue where an influx of neutrophils was observed on days 1 and 2 post infection [35]. When BAL cells were compared between mice infected with the gG deletion mutant and animals infected with a gG expressing virus, both the total number of immune cells as well as the percentage of neutrophils was significantly higher in the absence of the vCKBP. Interestingly, not only an effect on the migration of neutrophils between both groups of infected mice was observed, but there was also an effect on the influx of macrophages. At day 4 post infection, the percentage of macrophages was significantly lower in BAL cells from mice infected with the gG revertant virus. This observation is consistent with earlier findings that have shown that EHV-1

gG binds to a broad range of chemokines, including members of the C-C subfamily, which generally attract mononuclear cells [1].

In line with a previous study, it was observed that, especially at lower doses of infection ($<10^5$) and during the acute phase of infection, more severe clinical signs and a stronger inflammatory infiltration was observed in histological lung sections of mice infected with a gG-negative virus [13]. Following these initial observations, our data now clearly demonstrate that expression of EHV-1 gG can inhibit the recruitment of inflammatory cells *in vitro* and *in vivo*, which is in good agreement with what has been described for secreted vCKBP's of poxviruses [5]. As such, our data are the first to unravel the mechanisms of action of EHV-1 gG on murine chemokines *in vivo*, but it still remains elusive whether EHV-1 gG will display similar effects on inflammation and cell migration in its natural host, the horse. Future experiments are planned to close this gap and investigate the behaviour of gG negative mutants in horses.

Interference with chemokine signaling, thereby perturbing a fine-tuned network of the host's most immediate protection system, is one of the many defenses viruses use to evade or manipulate the host's arsenal to cope with intruders. In general, viruses must survive their encounter with the host's immune system to establish a successful infection. This requires that the virus avoids immediate immune elimination, but not to such an extent that the host succumbs to infection. With this in mind, it is reasonable to speculate that gG has played an important role in the establishment of a mutually acceptable relationship between virus and host that allows the virus to replicate, albeit at suboptimal levels, but at the same time does not cause too severe or even irreversible damage to the target host tissue. As such, alphaherpesvirus immune modulators might constitute a prerequisite for sustained maintenance within host populations and

play an essential role in the delicate co-evolutionary relationship between virus and target animal species.

Acknowledgments

The authors are grateful to Drs. Michael Studdert and Carol Hartley for supplying antibodies. We thank Jeremy Kamil and Neil Margulis for help with the baculovirus system and Patrick Smith for help with the BAL.

Reference List

1. Bryant, N. A., N. Davis-Poynter, A. Vanderplasschen, and A. Alcami. 2003. Glycoprotein G isoforms from some alphaherpesviruses function as broad-spectrum chemokine binding proteins. *EMBO J.* 22:833-846.

2. Costes, B., M. B. Ruiz-Arguello, N. A. Bryant, A. Alcami, and A. Vanderplasschen. 2005. Both soluble and membrane-anchored forms of Felid herpesvirus 1 glycoprotein G function as a broad-spectrum chemokine-binding protein. *J.Gen.Virol.* 86:3209-3214.

3. McFadden, G., A. Lalani, H. Everett, P. Nash, and X. Xu. 1998. Virus-encoded receptors for cytokines and chemokines. *Semin.Cell Dev.Biol.* 9:359-368.

4. Lusso, P. 2000. Chemokines and viruses: the dearest enemies. *Virology* 273:228-240.

5. Lalani, A. S., J. W. Barrett, and G. McFadden. 2000. Modulating chemokines: more lessons from viruses. *Immunol.Today* 21:100-106.

6. Parcells, M. S., S. F. Lin, R. L. Dienglewicz, V. Majerciak, D. R. Robinson, H. C. Chen, Z. Wu, G. R. Dubyak, P. Brunovskis, H. D. Hunt, L. F. Lee, and H. J. Kung. 2001. Marek's disease virus (MDV) encodes an interleukin-8 homolog (vIL-8): characterization of the vIL-8 protein and a vIL-8 deletion mutant MDV. *J.Virol.* 75:5159-5173.

7. Allen, G. P. and J. T. Bryans. 1986. Molecular epizootiology, pathogenesis, and prophylaxis of equine herpesvirus-1 infections. *Prog.Vet.Microbiol.Immunol.* 2:78-144.

8. van Maanen, C. 2002. Equine herpesvirus 1 and 4 infections: an update. *Vet.Q.* 24:58-78.

9. Patel, J. R. and J. Heldens. 2005. Equine herpesviruses 1 (EHV-1) and 4 (EHV-4)--epidemiology, disease and immunoprophylaxis: a brief review. *Vet.J.* 170:14-23.

10. Crabb, B. S. and M. J. Studdert. 1993. Epitopes of glycoprotein G of equine herpesviruses 4 and 1 located near the C termini elicit type-specific antibody responses in the natural host. *J.Virol.* 67:6332-6338.

11. Colle, C. F., III and D. J. O'Callaghan. 1995. Transcriptional analyses of the unique short segment of EHV-1 strain Kentucky A. *Virus Genes* 9:257-268.

12. Huang, J., C. A. Hartley, N. P. Ficorilli, B. S. Crabb, and M. J. Studdert. 2005. Glycoprotein G deletion mutants of equine herpesvirus 1 (EHV1; equine abortion virus) and EHV4 (equine rhinopneumonitis virus). *Arch.Virol.* 150:2583-2592.

13. von Einem, J., P. M. Smith, G. R. Van de Walle, D. J. O'Callaghan, and N. Osterrieder. 2007. In vitro and in vivo characterization of equine herpesvirus type 1 (EHV-1) mutants devoid of the viral chemokine-binding glycoprotein G (gG). *Virology*.

14. Drummer, H. E., M. J. Studdert, and B. S. Crabb. 1998. Equine herpesvirus-4 glycoprotein G is secreted as a disulphide-linked homodimer and is present as two homodimeric species in the virion. *J.Gen.Virol.* 79 (Pt 5):1205-1213.

15. Pycock, J. F., W. E. Allen, and T. H. Morris. 1987. Rapid, single-step isolation of equine neutrophils on a discontinuous Percoll density gradient. *Res.Vet.Sci.* 42:411-412.

16. Bennouna, S., W. Sukhumavasi, and E. Y. Denkers. 2006. Toxoplasma gondii inhibits toll-like receptor 4 ligand-induced mobilization of intracellular tumor necrosis factor alpha to the surface of mouse peritoneal neutrophils. *Infect.Immun.* 74:4274-4281.

17. Hubert, P. H., S. Birkenmaier, H. J. Rziha, and N. Osterrieder. 1996. Alterations in the equine herpesvirus type-1 (EHV-1) strain RacH during attenuation. *Zentralbl.Veterinarmed.B* 43:1-14.

18. Rudolph, J., D. J. O'Callaghan, and N. Osterrieder. 2002. Cloning of the genomes of equine herpesvirus type 1 (EHV-1) strains KyA and racL11 as bacterial artificial chromosomes (BAC). *J.Vet.Med.B Infect.Dis.Vet.Public Health* 49:31-36.

19. Benarafa, C., F. M. Cunningham, A. S. Hamblin, D. W. Horohov, and M. E. Collins. 2000. Cloning of equine chemokines eotaxin, monocyte chemoattractant protein (MCP)-1, MCP-2 and MCP-4, mRNA expression in tissues and induction by IL-4 in dermal fibroblasts. *Vet.Immunol.Immunopathol.* 76:283-298.

20. Kamil, J. P., B. K. Tischer, S. Trapp, V. K. Nair, N. Osterrieder, and H. J. Kung. 2005. vLIP, a viral lipase homologue, is a virulence factor of Marek's disease virus. *J.Virol.* 79:6984-6996.

21. von Einem, J., J. Wellington, J. M. Whalley, K. Osterrieder, D. J. O'Callaghan, and N. Osterrieder. 2004. The truncated form of glycoprotein gp2 of equine herpesvirus 1 (EHV-1) vaccine strain KyA is not functionally equivalent to full-length gp2 encoded by EHV-1 wild-type strain RacL11. *J.Virol.* 78:3003-3013.

22. Smith, P. M., Y. Zhang, W. D. Grafton, S. R. Jennings, and D. J. O'Callaghan. 2000. Severe murine lung immunopathology elicited by the pathogenic equine herpesvirus 1 strain RacL11 correlates with early production of macrophage inflammatory proteins 1alpha, 1beta, and 2 and tumor necrosis factor alpha. *J.Virol.* 74:10034-10040.

23. Baggiolini, M. 1998. Chemokines and leukocyte traffic. *Nature* 392:565-568.

24. Fiebich, B. L., B. Jager, C. Schollmann, K. Weindel, J. Wilting, G. Kochs, D. Marme, H. Hug, and H. A. Weich. 1993. Synthesis and assembly of functionally active human vascular endothelial growth factor homodimers in insect cells. *Eur.J.Biochem.* 211:19-26.

25. Telford, E. A., M. S. Watson, J. Perry, A. A. Cullinane, and A. J. Davison. 1998. The DNA sequence of equine herpesvirus-4. *J.Gen.Virol.* 79 (Pt 5):1197-1203.

26. Luscinskas, F. W., J. M. Kiely, H. Ding, M. S. Obin, C. A. Hebert, J. B. Baker, and M. A. Gimbrone, Jr. 1992. In vitro inhibitory effect of IL-8 and other chemoattractants on neutrophil-endothelial adhesive interactions. *J.Immunol.* 149:2163-2171.

27. Zlotnik, A. and O. Yoshie. 2000. Chemokines: a new classification system and their role in immunity. *Immunity.* 12:121-127.

28. Lin, M., E. Carlson, E. Diaconu, and E. Pearlman. 2006. CXCL1/KC and CXCL5/LIX are produced selectively by corneal fibroblasts and mediate neutrophil infiltration to the corneal stroma in LPS keratitis. *J.Leukoc.Biol.*

29. Devlin, J. M., G. F. Browning, C. A. Hartley, N. C. Kirkpatrick, A. Mahmoudian, A. H. Noormohammadi, and J. R. Gilkerson. 2006. Glycoprotein G is a virulence factor in infectious laryngotracheitis virus. *J.Gen.Virol.* 87:2839-2847.

30. Oakes, J. E., C. A. Monteiro, C. L. Cubitt, and R. N. Lausch. 1993. Induction of interleukin-8 gene expression is associated with herpes simplex virus infection of human corneal keratocytes but not human corneal epithelial cells. *J.Virol.* 67:4777-4784.

31. Inagi, R., R. Guntapong, M. Nakao, Y. Ishino, K. Kawanishi, Y. Isegawa, and K. Yamanishi. 1996. Human herpesvirus 6 induces IL-8 gene expression in human hepatoma cell line, Hep G2. *J.Med.Virol.* 49:34-40.

32. Pusterla, N., W. D. Wilson, P. A. Conrad, S. Mapes, and C. M. Leutenegger. 2006. Comparative analysis of cytokine gene expression in cerebrospinal fluid of horses without neurologic signs or with selected neurologic disorders. *Am.J.Vet.Res.* 67:1433-1437.

33. Legler, D. F., M. Loetscher, R. S. Roos, I. Clark-Lewis, M. Baggiolini, and B. Moser. 1998. B cell-attracting chemokine 1, a human CXC chemokine expressed in lymphoid tissues, selectively attracts B lymphocytes via BLR1/CXCR5. *J.Exp.Med.* 187:655-660.

34. Shanley, J. D. and Z. K. Ballas. 1985. Alteration of bronchoalveolar cells during murine cytomegalovirus interstitial pneumonitis. *Am.Rev.Respir.Dis.* 132:77-81.

35. Bartels, T., F. Steinbach, G. Hahn, H. Ludwig, and K. Borchers. 1998. In situ study on the pathogenesis and immune reaction of equine herpesvirus type 1 (EHV-1) infections in mice. *Immunology* 93:329-334.

Footnotes

1. **Correspondence address:** Nikolaus Osterrieder, Department of Microbiology and Immunology, College of Veterinary Medicine, Cornell University, Ithaca, NY 14853. phone: (607) 253-4045, FAX: (607) 253-3384, e-mail: no34@cornell.edu.
2. **Source of support:** This study was supported by a grant from the Harry M. Zweig Memorial Fund for Equine Research at Cornell University.
3. **Special abbreviations:** gG: glycoprotein G; vCKBP: viral chemokine binding protein; EHV-1: equine herpesvirus type 1; EHV-4; equine herpesvirus type 4; p.i.: post infection; vL11ΔgG: gG deletion mutant of RacL11; vL11ΔgG: gG rescuant virus of RacL11; sgG-His: His-tagged secreted gG; BAL: bronchioalveolar lavage

Figure Legends

Figure 1. Generation of pBac11sgG. (A). Overall genome organization of the bacterial artificial chromosome (BAC) pRacL11 consisting of a unique-long (U_L) and a unique-short (U_S) segment, bracketed by inverted internal repeat (IR) and terminal repeat (TR) sequences. **(B).** Organization of the unique-short segment, depicted in (A). **(C).** Schematic representation of gene 70 (gG) with restriction enzyme sites for cloning in pBac11 using primers as described in Table 1 (TM: transmembrane domain; C: CpoI). **(D).** Schematic representation of the pBac11sgG containing the extracellular domain of gG in frame with the gp64 signal peptide, with a Histag attached at the carboxyterminus end of gG.

Figure 2. (A). Chemotaxis assays studying IL-8-induced migration of equine immune cells. For neutrophils, chemotaxis was performed using 3μM pore size Transwell plates with the indicated concentrations of equine IL-8 at 37°C for 45min, for equine PBMC 5μM pore size Transwell plates were used and the incubation was increased to 2h. Data are expressed as the mean ± SEM of at least 3 independent experiments. **(B). Supernatant of EHV-1-infected cells inhibits IL-8-induced chemotaxis of equine neutrophils.** Chemotaxis assays with equine neutrophils and equine IL-8 were performed with 300μl supernatant of mock-infected (white bars) or EHV-1-infected cells (grey bars). Data are expressed as the mean ± SEM of at least 3 independent experiments.

Figure 3. IL-8-induced chemotaxis of equine neutrophils is not altered in the absence of secreted gG in supernatant of EHV-1-infected cells. (A). Cell- and virion-free supernatants of EHV-1 wild type (WT), vL11ΔgG- or vL11ΔgGR-infected cells were separated by SDS-12% PAGE, transferred to a nitrocellulose membrane and incubated with anti-EHV-1 gG antibodies

(1:500). Supernatant of mock-infected cells was included as a negative control. **(B)**. Chemotaxis assays with equine neutrophils were performed with IL-8 alone (black bars), 300µl supernatant of EHV-1 WT- (white bars), vL11ΔgG- (grey bars) or vL11ΔgGR-infected cells (striped bars). Data are expressed as the mean ± SEM of at least 3 independent experiments. Asteriks indicate a significant difference compared to IL-8 alone. The 100% response equals 42±5.2% and 54±3.7% chemotaxis for 25ng/ml and 50ng/ml IL-8 respectively.

Figure 4. Glycoprotein G of EHV-1 is responsible for the inhibition of IL-8-induced chemotaxis of equine neutrophils. (A). Secreted gG-His (sgG-His) from a baculovirus expression system was purified with TALON columns and the different elution fractions were separated by SDS-10% PAGE and stained with Coomassie blue. The left panel represents elution fraction, while the right panel depicts results of a western blot where sgG-His was detected using polyclonal anti-gG antibodies: 1, supernatant mock-infected cells; 2, supernatant mock-infected Sf9 insect cells; 3, supernatant EHV-1-infected cells; 4, purified sgG-His. **(B).** Chemotaxis assays with equine neutrophils and 50ng/ml equine IL-8 were performed with increasing concentrations of purified sgG of EHV-1. Data are expressed as the mean ± SEM of at least 3 independent experiments. The 100% response equals 42±5.7% chemotaxis.

Figure 5. Supernatant of EHV-4 does not interfere with IL-8-induced chemotaxis of equine neutrophils. (A). Chemotaxis assays with equine neutrophils and 50ng/ml equine IL-8 were performed with increasing concentrations of supernatant of EHV-4- infected cells. Data are expressed as the mean ± SEM of at least 3 independent experiments. The 100% response equals 47±7.3% chemotaxis. **(B).** Cell- and virion-free supernatants of EHV-4-, EHV-1- or mock-infected cells were separated by SDS-12% PAGE, transferred to a nitrocellulose membrane and incubated with anti-EHV-4 gG antibodies (1:500).

Figure 6. Supernatant of EHV-1-infected cells does not interfere with CCL-2--induced chemotaxis of equine monocytes. (A) Cell-free supernatant from Sf9 insect cells infected with eCCL-2-His recombinant baculovirus was prepared and separated by SDS-10% PAGE, transferred to a nitrocellulose membrane and incubated with anti-Penta-His antibodies (1:1000). This resulted in a major protein band with a size of approximately 10kDa (lane 2, indicated with an asteriks). Lane 1 is supernatant from mock-infected insect cells. **(B.)** Chemotaxis was performed using 5μM pore size Transwell plates with the indicated dilutions of supernatant containing equine CCL-2 at 37°C for 2h. Data are expressed as the mean ± SEM of at least 3 independent experiments. **(C)** Chemotaxis assays with equine monocytes and the indicated supernatant dilution containing equine CCL-2 were performed in the presence (grey bars) or absence (white bars) of 0.6μg/ml sgG-His. Data are expressed as the mean ± SEM of at least 3 independent experiments.

Figure 7. Pathogenesis of EHV-1 infection in a murine infection model in the absence of gG. (A). Mice in groups of sixteen were infected intranasally with 10^4 PFU of vL11ΔgGR (Δ), vL11ΔgG (□), or mock-infected (◊). Mean body weights were determined on the day of infection (day 0) up to day 14 post infection (p.i.). Mean body weights and STDEV are shown. Asteriks indicate statistically significant differences ($p<0.05$) between vL11ΔgGR- and vL11ΔgG-inoculated mice. **(B).** Viral titers were determined in 2 mice of each group at day 1, 2 and day 4 p.i. Titers in lungs of vL11ΔgGR- (black bars) or vL11ΔgG-inoculated mice (white bars) and STDEV are shown. The limit of detection was 10^1 PFU/mg lung and the cases where no virus from lungs was recovered are indicated by <1 (control mice). Asteriks indicate statistically significant differences ($p<0.05$).

Figure 8. (A). Glycoprotein G of EHV-1 inhibits KC-induced chemotaxis of murine neutrophils. Chemotaxis assays with murine neutrophils were performed with 0.1µg/ml of murine KC, pre-incubated with 300µl supernatant of mock-infected, vL11ΔgGR- or vL11ΔgG-infected cells. Data are expressed as the mean ± SEM of at least 3 independent experiments. The 100% response equals 37±8.4% chemotaxis. **(B). In vivo relevance of gG on the influx of immune cells in a murine model of EHV-1 infection.** Total amount of immune cells from mice infected intranasally with vL11ΔgGR (white bars) or vL11ΔgG (grey bars), or mock-infected (black bars). At different days post infection (p.i.), inflammatory cells were harvested by bronchioalveolar lavage (BAL), washed and counted. Data are presented as the mean ± SEM and asteriks indicate statistically significant differences ($p < 0.05$).

Figure 9. In vivo relevance of gG on neutrophil migration in a murine model of EHV-1 infection. (A). Absolute number of neutrophils in BAL cells of mice infected intranasally with vL11ΔgGR (white bars) or vL11ΔgG (grey bars), or mock-infected (black bars). At different days p.i., BAL cells were harvested, stained and the number of neutrophils were determined. Data are presented as the mean ± SEM and asteriks indicate statistically significant differences ($p < 0.01$). **(B).** Flowcytometric analysis of BAL cells of mice infected intranasally with vL11ΔgGR, vL11ΔgG or mock-infected. At day 2 p.i. BAL cells from at least 4 mice per group were pre-incubated with normal mouse serum for 30min at 4°C and subsequently stained with labeled antibodies against cells of the innate immune system or the adaptive immune system for 15min at 4°C (a). Representative flowcytometric histograms showing the percentage of neutrophils for each group of infected mice (b).

Table 1. Primers used in this study

primer	**sequence**[a]
gGFCpo	5’ -atgccggtccgatggccccagatgaactctgttatg- 3’
gGRCpo	5’ -acgtcggaccggcggcatacacagttttgagc- 3’
CCL2FCpo	5’ -agccggtccgatgaaggtctctgcagcc- 3’
CCL2RCpo	5’ -agctcggaccggcaggctttggagtttgggc- 3’

[a]Underlined nucleotides indicate the CpoI sequence, used for cloning into the pFastBac

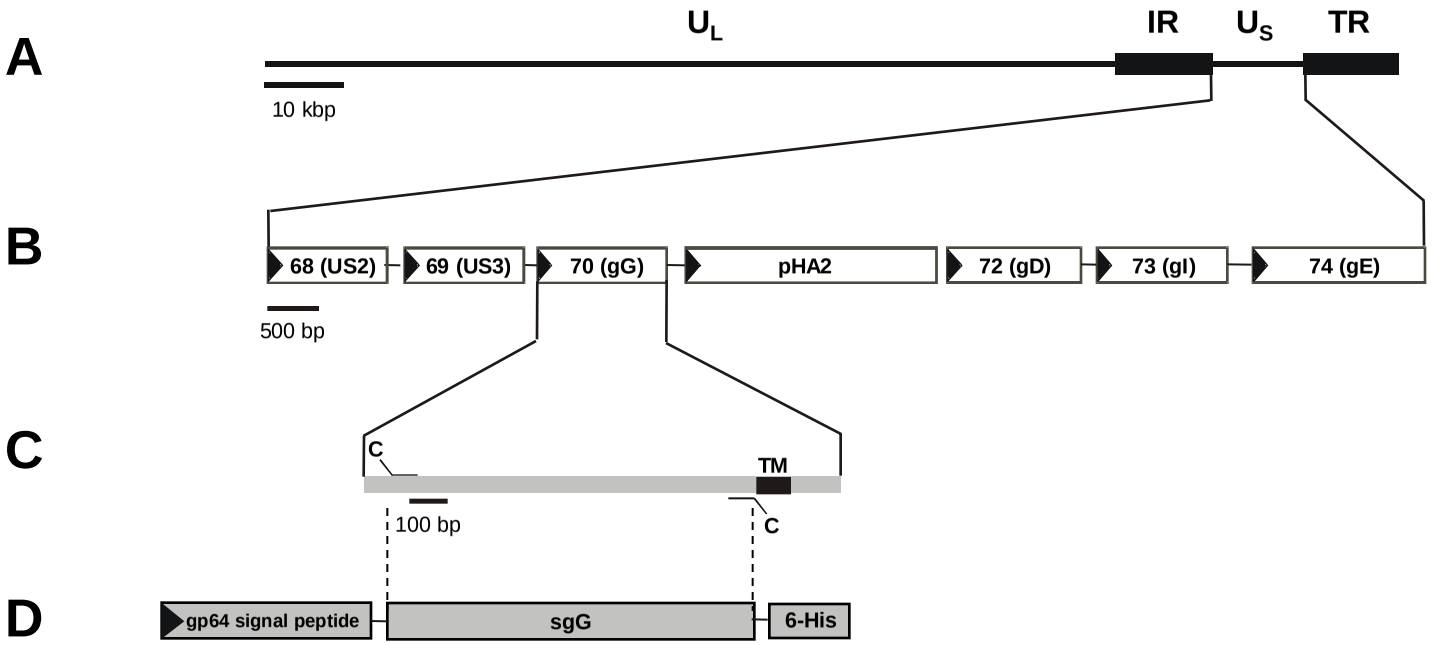

Figure 1: Van de Walle *et al.*

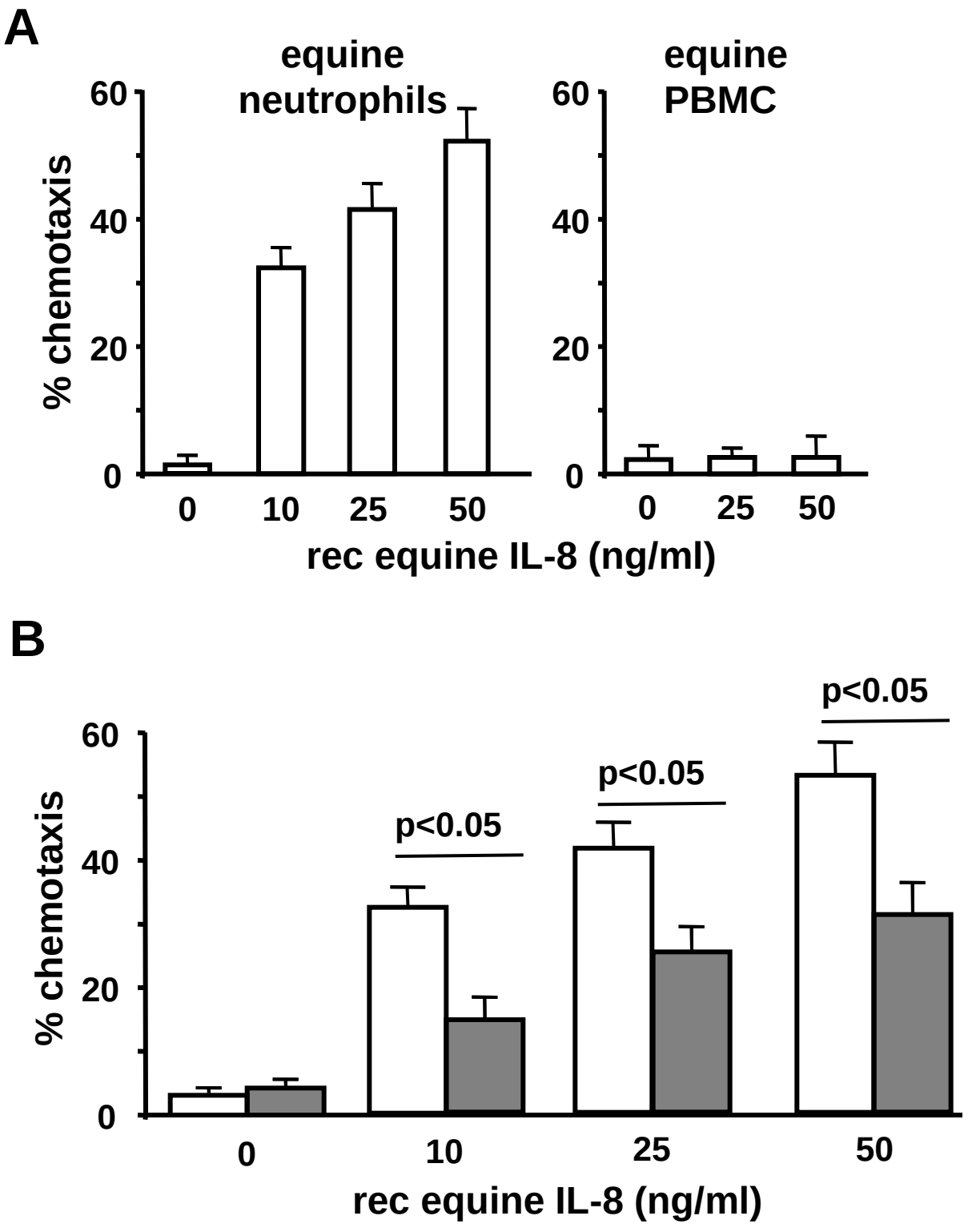

Figure 2: Van de Walle *et al.*

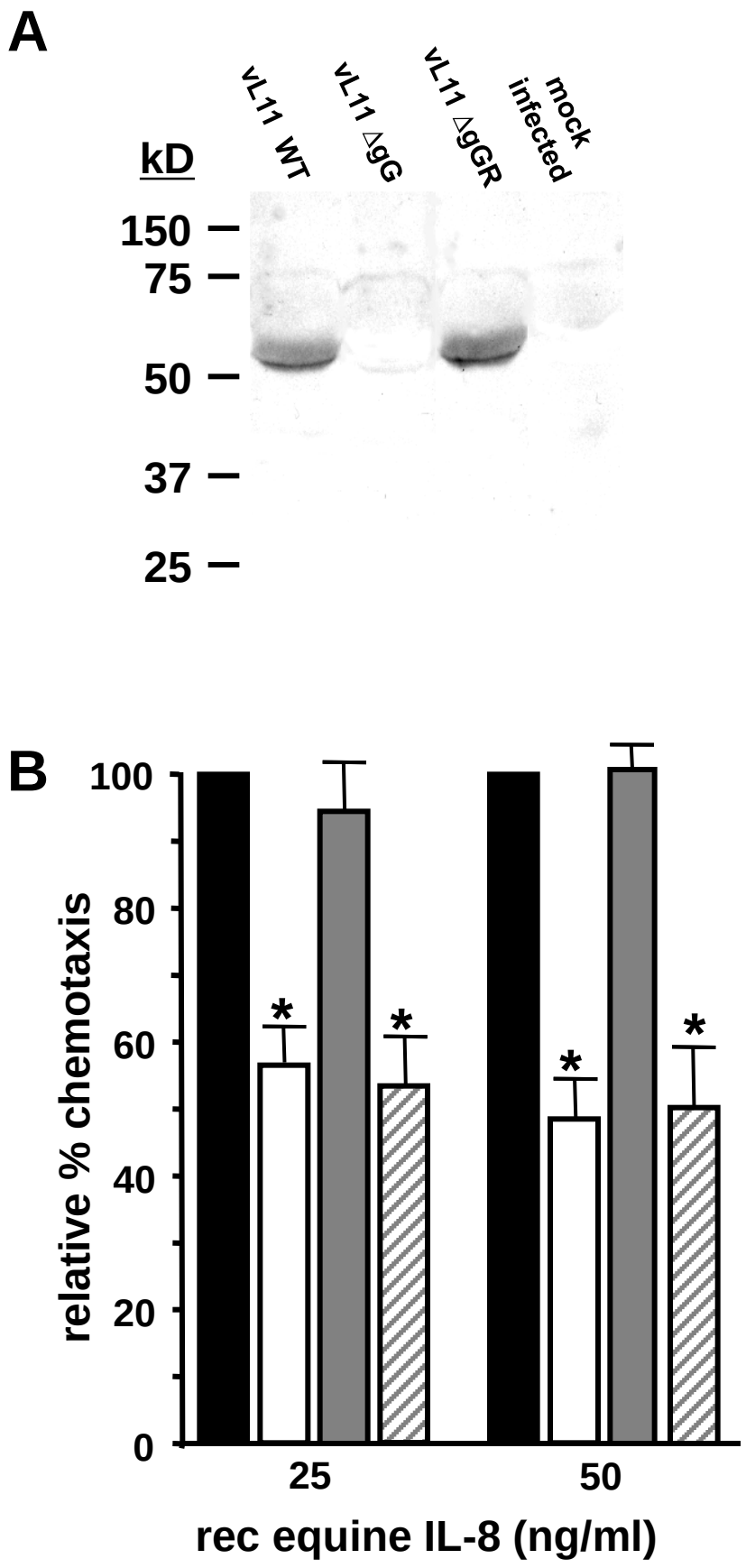

Figure 3: Van de Walle *et al.*

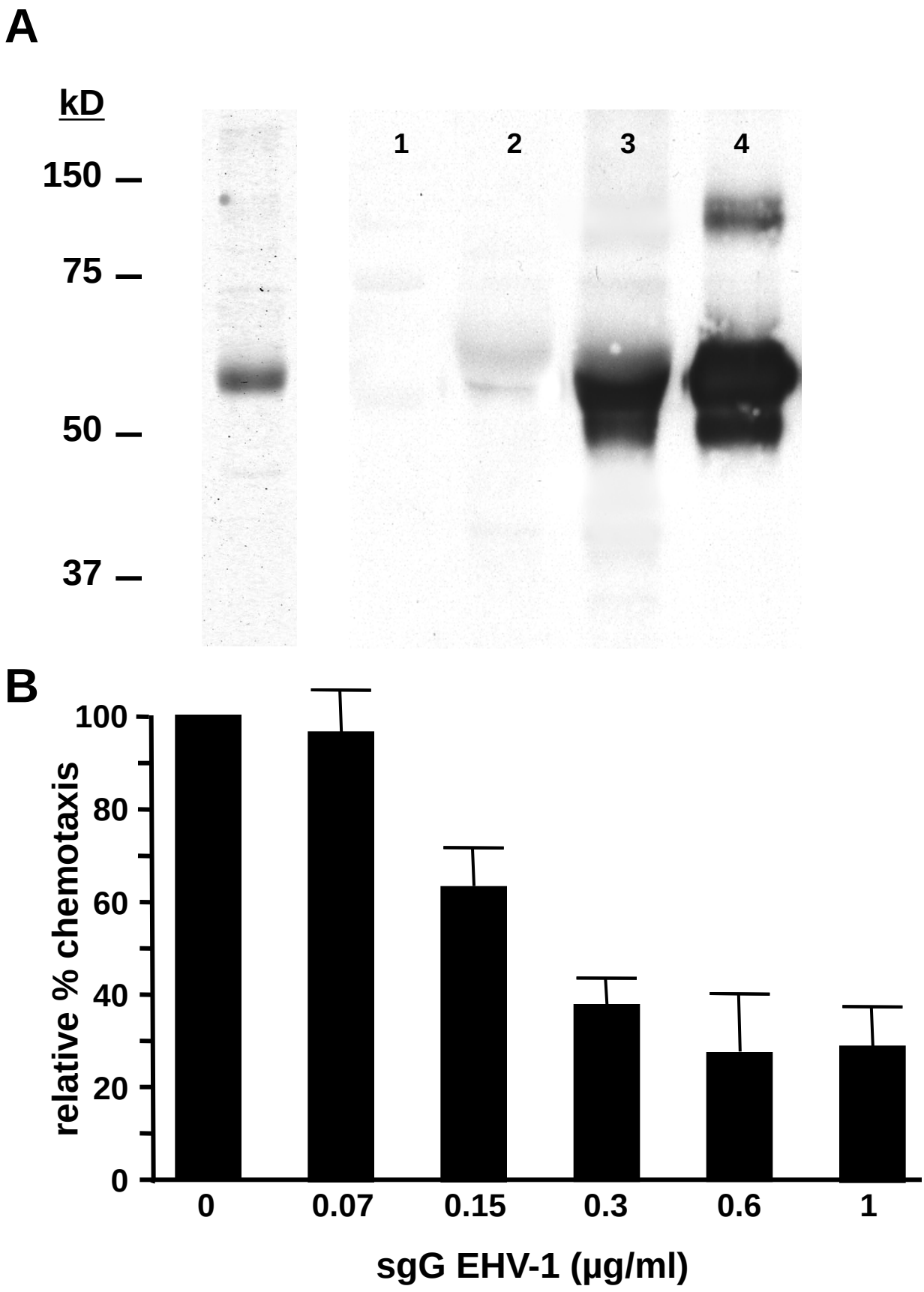

Figure 4: Van de Walle *et al.*

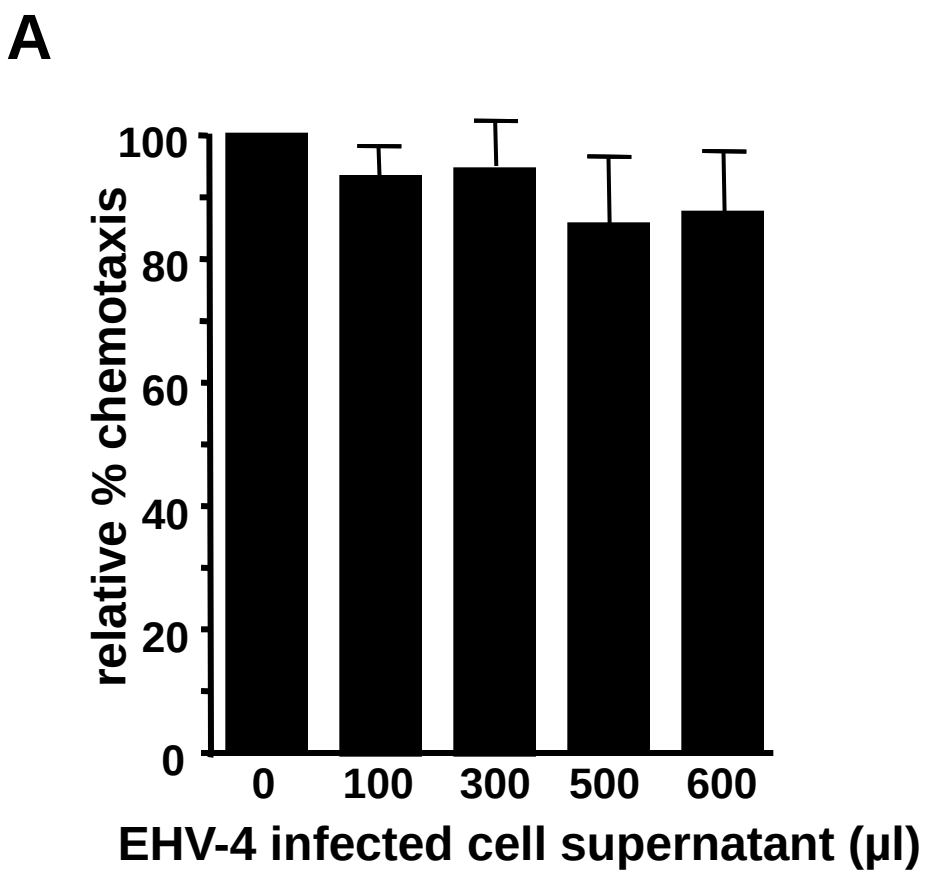

Figure 5: Van de Walle *et al.*

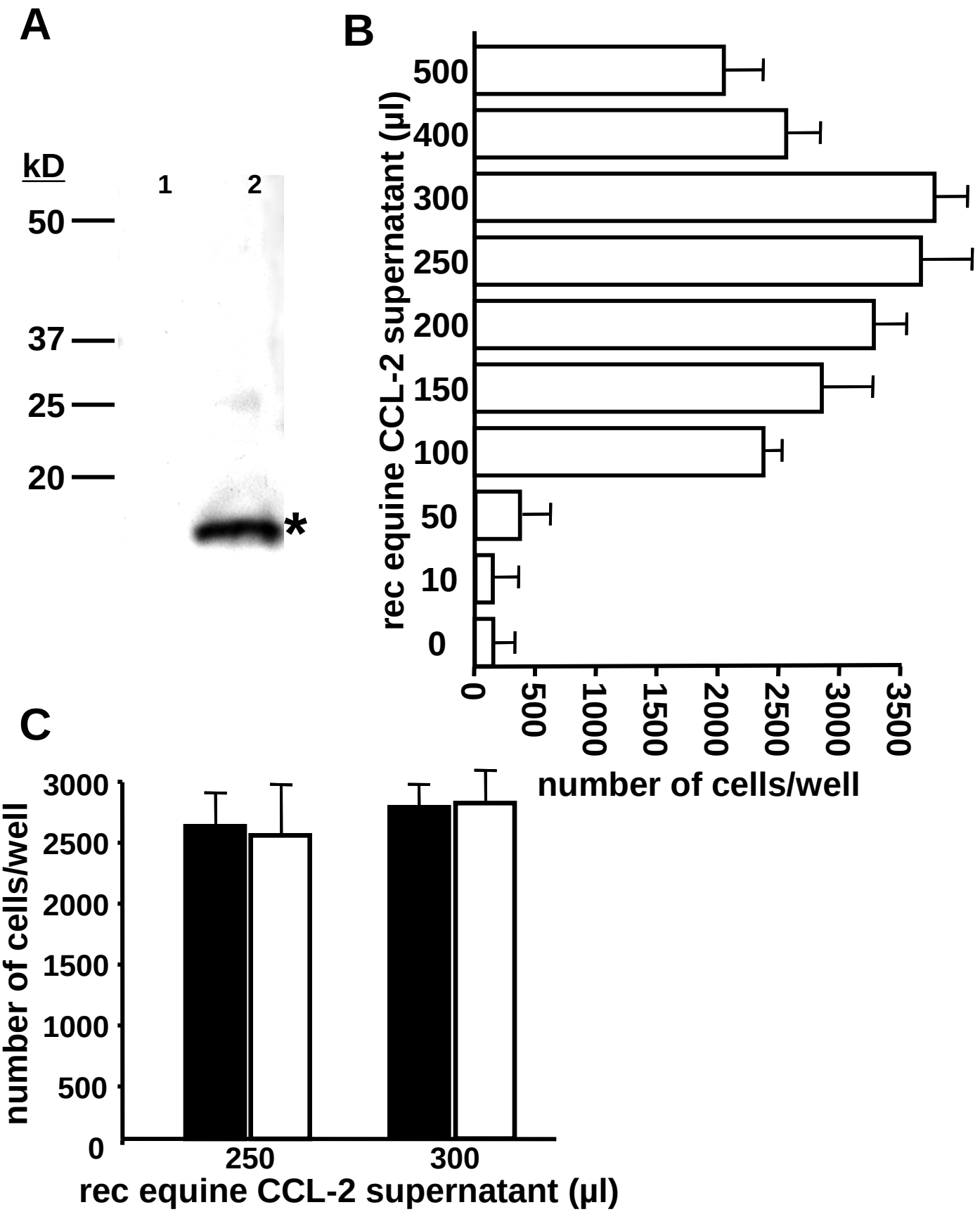

Figure 6: Van de Walle *et al.*

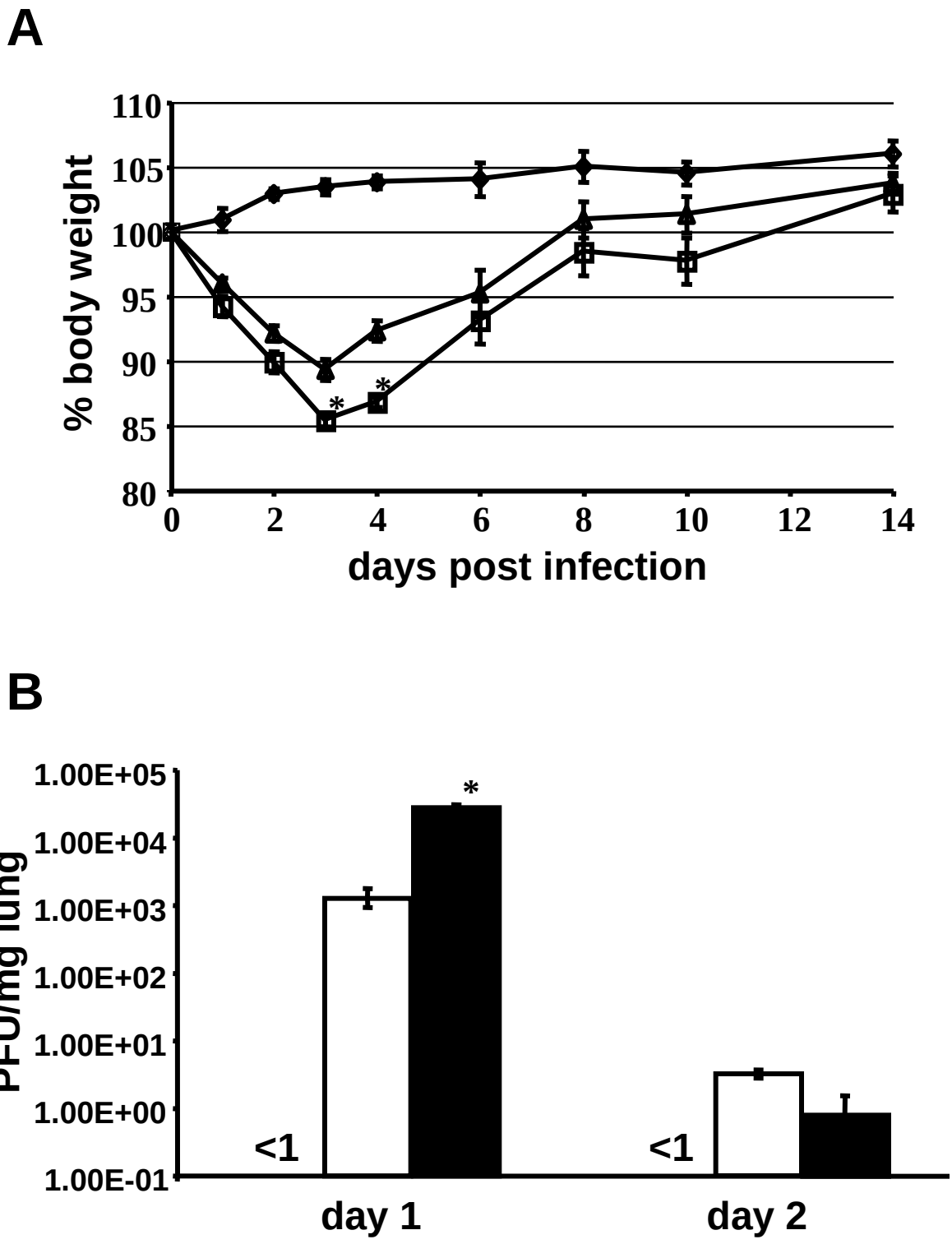

Figure 7: Van de Walle *et al.*

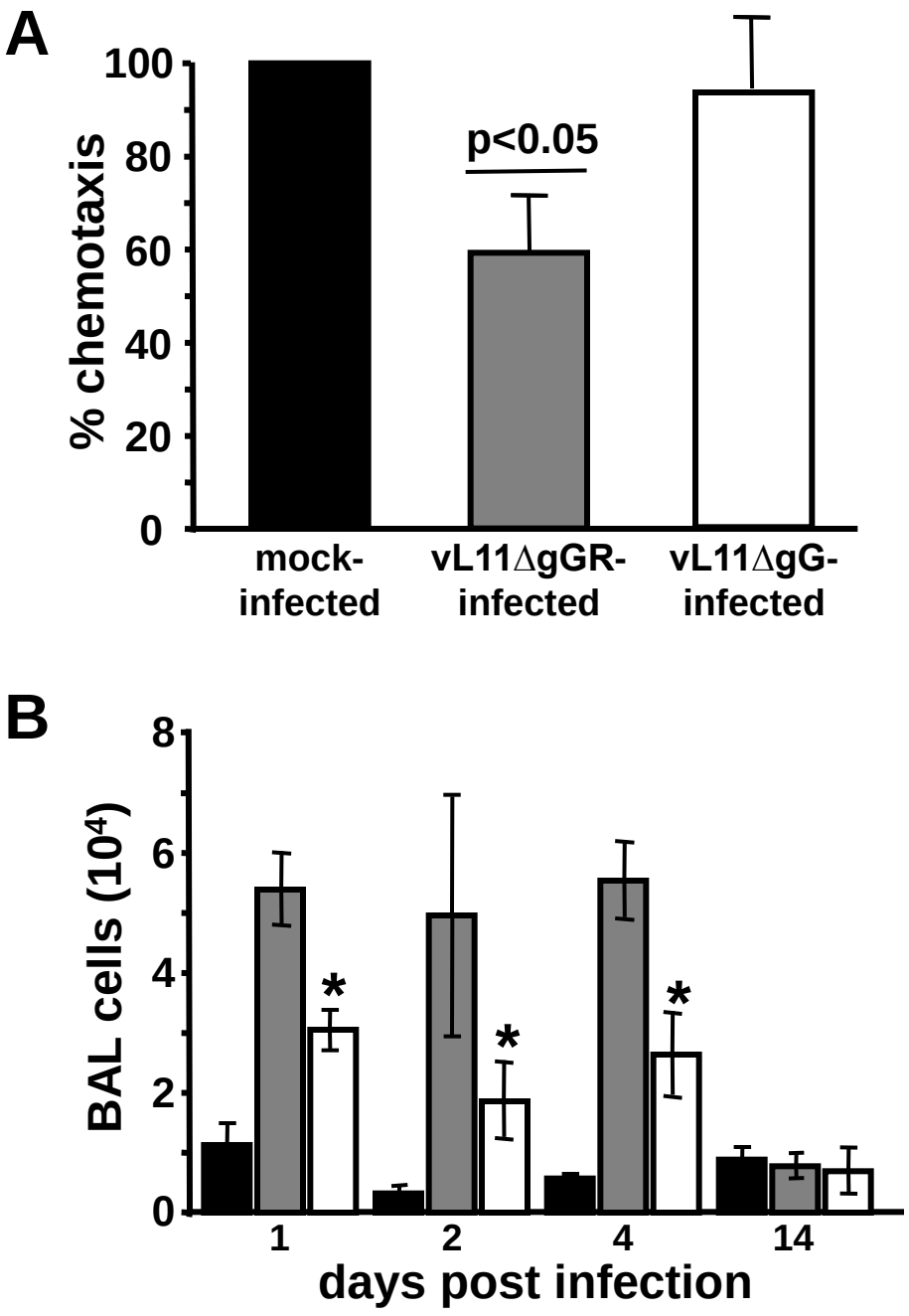

Figure 8: Van de Walle *et al.*

A

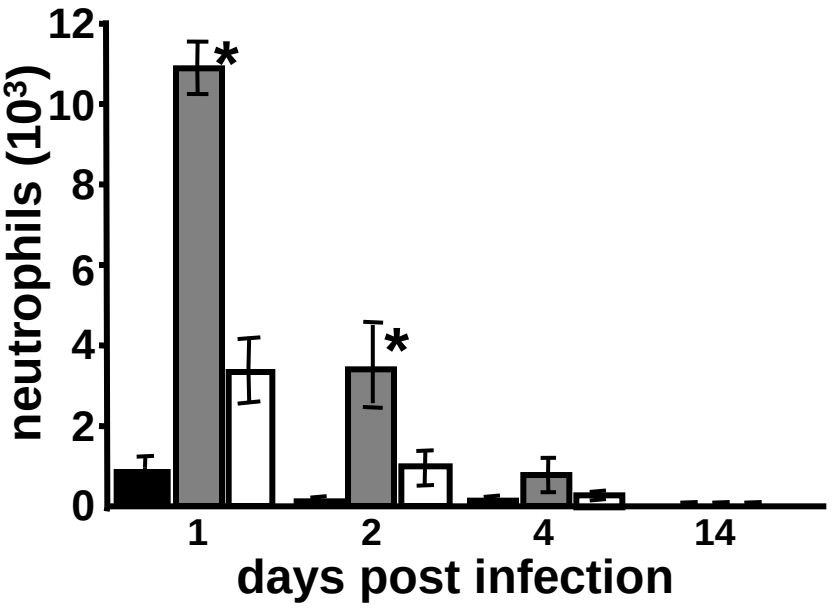

B

(a)

marker	cell type	% of positive cells upon infection with		
		mock	vL11ΔgGR	vL11ΔgG
$Gr1^+$	neutrophil	3.0	11.6	24.4
F4/80	macrophage	0.7	7.8	8.3
B220	B lymphocyte	11.8	34.1	28.5
CD3	T lymphocyte	33.1	47.7	45.5

(b)

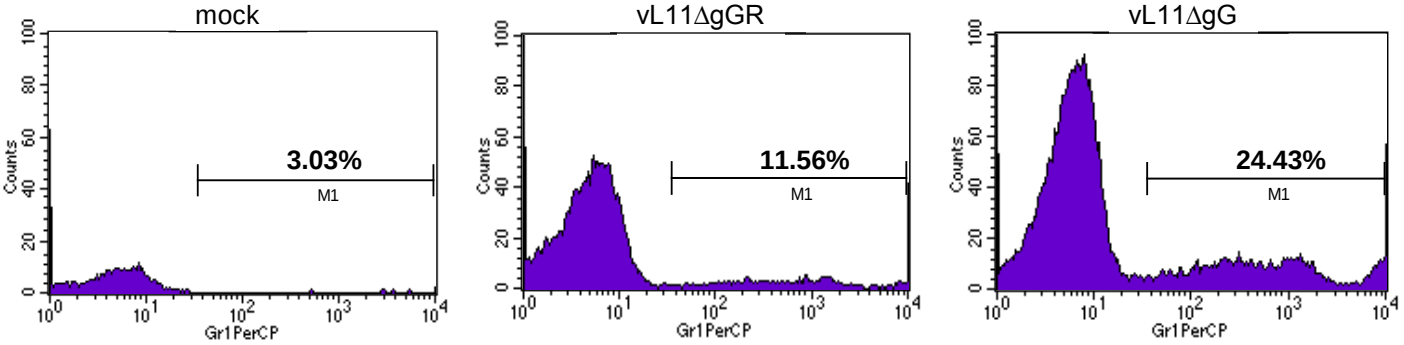

Figure 9: Van de Walle *et al.*